

Time structure measurement of the SSRF storage ring using TRXEOL method*ZHANG Zhao-Hong (张招红),^{1,2} JIANG Zheng (姜政),¹ XUE Song (薛松),¹ and ZHENG Li-Fang (郑丽芳)^{1,†}¹*Shanghai Institute of Applied Physics, Chinese Academy of Sciences, Shanghai 201204, China*²*University of Chinese Academy of Sciences, Beijing 100049, China*

(Received October 24, 2014; accepted in revised form December 8, 2014; published online July 21, 2015)

In order to do alignment between the timing signal and the synchrotron X-ray pulse on the sample spot in the time domain, measuring time structure of the storage ring on the sample spot inside the experimental hutch is a foundational step during the time-resolved experiments using the pulsed synchrotron X-rays with the time structure defined by the storage ring. In this work, the method of time-resolved X-ray excited optical luminescence (TRXEOL) was designed and implemented to do the measurement. It is based on the principle of time-correlated single photon counting techniques. The measurement system consists of a spectrometer with a detector of photomultiplier tube, a timing system, a set of nuclear instrument modules and a luminescent material of zinc oxide. The measurement was performed on the X-ray absorbed fine structure spectrum beamline at Shanghai Synchrotron Radiation Facility. The results show that this method can be used to measure the time structure of the storage ring with a precision of less than 1 ns. The measurement system can also be used for the time-resolved research for the optical luminescent materials.

Keywords: Synchrotron ring time structure, X-ray excited optical luminescence, Time-resolved X-ray excited optical luminescence, Shanghai Synchrotron Radiation Facility

DOI: [10.13538/j.1001-8042/nst.26.040202](https://doi.org/10.13538/j.1001-8042/nst.26.040202)**I. INTRODUCTION**

The 432-m storage ring of Shanghai Synchrotron Radiation Facility (SSRF) has a time width of 1440 ns which is divided into 720 filling buckets [1], each being filled with a single electron bunch, which has a time width of less than 100 ps. So the width of X-ray pulses along the beamline produced by corresponding electron bunches is less than 100 ps, and the shortest time interval between two consecutive pulses is 2 ns. As a great advantage, the time structure of pulsed X-rays allows many time-resolved experiment methods to be implemented [2].

In a time-resolved experiment [3], for aligning the timing signal and synchrotron X-ray pulse on the sample spot in the time domain, time structure of the storage ring must be measured accurately on the sample spot inside the experiment hutch, so as to obtain time structure of the X-ray pulses produced by electron bunches. A traditional method is to set a fast photodiode on the sample spot [4]. Every time an X-ray pulse arrives, the photodiode produces an electrical pulse. The time structure is acquired by recording the electrical pulses in the time domain. An ultrahigh performance oscilloscope is needed. In pump-probe nanosecond time-resolved luminescent experiments [5], a single X-ray pulse induced by a single electron bunch is used as the pump source, some electronic instruments are used to detect signals in the dark time of several hundred nanoseconds after the single X-ray pulse. Luminescent decays involve a broad range of life times ranging from nanoseconds to milliseconds [6]. So, achieving nanosecond time resolution is sufficient in this kind of experiments. However, in the phase-II project of SSRF,

hundred-picosecond time-resolved experiment has been proposed. To accommodate this, the ring time structure must be measured with a resolution less than 100 picoseconds by using an avalanche photodiode to detect the X-rays [7].

In this paper, time-resolved X-ray excited optical luminescence (TRXEOL) [8] method is implemented to measure time structure of the storage ring. XEOL describes the photon emission after absorption of synchrotron X-rays [9]. In a TRXEOL cycle, the sample is excited by a single X-ray pulse, the emitted photons are detected and recorded before next X-ray pulse comes. The method is based on the principle of time-correlated single photon counting techniques (TCSPC) [10]. The measurement system consists of a spectrometer with a detector and photomultiplier tube (PMT), a timing system, a set of nuclear instrument modules (NIM), and a fast optical luminescent (< 1 ns, at 390 nm) material of ZnO [11, 12]. The time structure of the ring is indirectly measured by detecting and recording the timestamps of the luminescent pulses. The measurements performed on the X-ray absorption fine structure spectroscopy (XAFS) beamline (BL14W1 [13]) show that time resolution of the measurement system is < 1 ns.

II. PRINCIPLE OF THE MEASUREMENT**A. Time structure of the storage ring**

As shown in Fig. 1, the SSRF storage ring has four filling patterns: single bunch pattern, multi-bunch pattern, hybrid filling pattern and full filling pattern. After its Phase-II project, SSRF will be able to perform 100 ps resolution pump-probe experiments in its hybrid filling pattern, in which a single electron bunch is filled into a specific bucket, and a serial of multiple bunches is filled into some consecutive buckets.

* Supported by the 973 Program (No. 2010CB934501)

† Corresponding author, zhenglifang@sinap.ac.cn

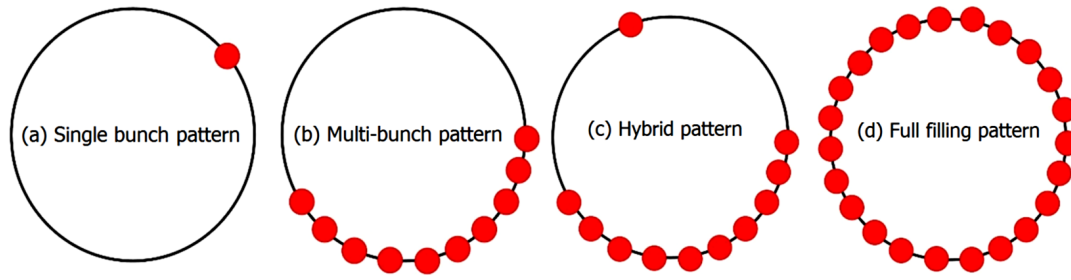


Fig. 1. (Color online) Filling patterns of the SSRF storage ring (RF, 499.654 MHz; 720 buckets).

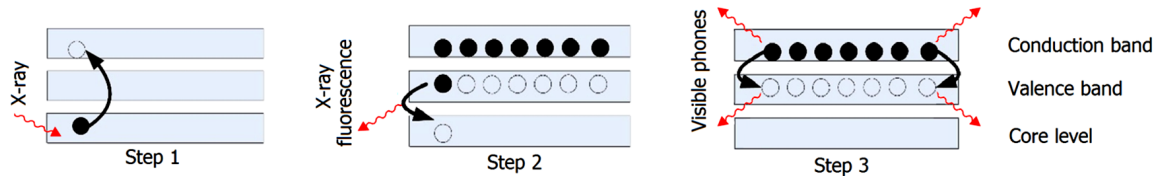


Fig. 2. (Color online) Schematics of the XEOL process in luminescent material.

The time interval between the single bunch and the multiple bunches can be adjusted by changing the number and position of the multiple bunches. Dark time gaps on both sides of the single bunch range from 2 to 1440 ns.

B. Interactions between X-rays and luminescent material

XEOL is a complex process of interactions between X-rays and luminescent material [14]. As shown in Fig. 2, Step 1 is creation of the core holes and more electrons in the conduction band, taking place within femtoseconds [8]. In Step 2, the electrons from the valence band fill into the core hole with X-ray fluorescence or Auger decay which generates additional holes in the valence band. Step 2 is also ultra-fast process. In Step 3, the electrons in the conduction band and the holes in the valence band resulting from secondary processes recombine and generate optical luminescence.

TRXEOL monitors the optical luminescent lifetime [15]. The luminescent decays involve a wide range of lifetimes which range from nanoseconds to milliseconds [14]. If a material of < 200 ns optical luminescent lifetime can be used as a sensor to detect the luminescence emitted from the sample excited by the pulsed X-rays, time structure of the storage ring will be measured properly, because the electron bunch is of about 100 ps width and the minimum interval between two consecutive electron bunches is 2 ns.

C. Theory of the detection of the luminescence

In an excitation circle, the X-ray pulse hits the sample of ZnO nanowire, the sample emits optical luminescence, and the PMT and the electrics detect and record decay process of the optical luminescence. After plenty of repeated circles, the time structure is obtained indirectly after statistical analysis

of the data of optical luminescence decay processes. This method is based on the TCSPC technique.

TCSPC measures the luminescence lifetime in essence. As shown in Fig. 3, the trigger pulse is synchronized with the X-ray pulse, so it is used to indicate the time when the X-ray pulse hits the sample and as the START input of the time-to-amplitude converter (TAC). The PMT outputs an electrical pulse every time a photon is detected from the spectrometer. This electrical pulse is fed to STOP input of the TAC. The TAC converts the time interval between the START and STOP pulses to a proportional amplitude of voltage. In each excitation circle, once the detector outputs a valid pulse, the multichannel analyzer (MCA) regards that a single photon is detected and a single count is registered in the corresponding time channel, i.e., the MCA does not take into account the pulse size. The MCA generates an array of numbers of detected photons within short time intervals after plenty of excitation circles. A photon arrival histogram, which represents the luminescent decay curve of the sample, can be obtained with this numerical array.

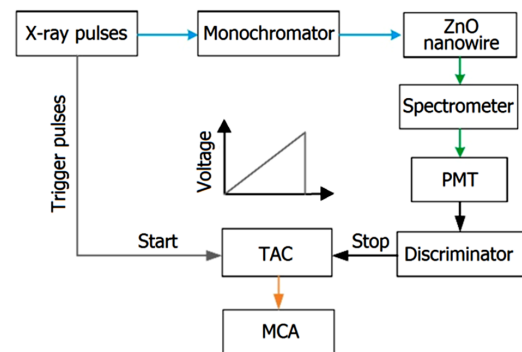


Fig. 3. (Color online) Schematics of the TCSPC method.

Supposing the interval of one MCA channel is $t_i + \Delta t$, the

average number of photons (w_i) reaching the detector within each interval $t_i + \Delta t$ should be less than one, because the events are pulsed weak nuclear processes. The probability of z photons reaching the detector in each interval is given by Poisson distribution

$$p_i(z) = \frac{w_i^z}{z!} \exp(-w_i). \quad (1)$$

Specifically

$$\begin{aligned} p_i(0) &= \exp(-w_i), \\ p_i(1) &= w_i \exp(-w_i), \\ p_i(z > 1) &= 1 - p_i(0) - p_i(1) \\ &= 1 - (1 + w_i) \exp(-w_i). \end{aligned} \quad (2)$$

After many (N_E) excitation circles, N_i counts will be detected in the i^{th} interval.

$$N_i \cong N_E [p_i(1) + p_i(z > 1)]. \quad (3)$$

$w_i \ll 1$, therefore

$$\begin{aligned} p_i(1) &\cong w_i; \quad p_i(z > 1) \cong w_i^2, \\ N_i &\cong N_E [w_i + w_i^2] \cong N_E w_i. \end{aligned} \quad (4)$$

N_E is a constant, so the counts in the i^{th} interval is indeed proportional to the intensity in the interval ($t_i + \Delta t$). And the shape of histogram in the MCA software is approximately equal to the theoretical optical luminescence curve.

III. THE MEASUREMENT SETUP

The measurement setup (Fig. 4) includes a spectrometer, a timing system, an NIM system and a ZnO material.

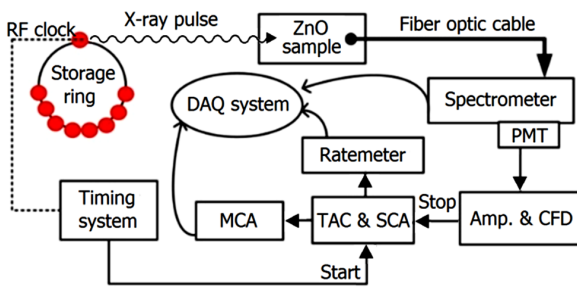


Fig. 4. (Color online) Schematics of the setup.

A. Timing system

The timing system produces a high precision trigger pulse synchronized with the X-ray pulse at the sample spot to indicate the start time when the X-ray pulse hits the sample. Designed based on VEM bus, FPGA and high-speed serial communication technology, it contains the timing event generator

(EVG) module, fanout modules, timing event receiver (EVE) modules and optical fiber transmission network [16]. The reference clock source of the EVG is the 500 MHz radio frequency (RF) clock of the SSRF accelerators. Timing events and trigger clocks are generated in the EVG and coded to serial frames according to 8b10b protocol. The coded frames are transmitted on the fiber network. The fanout modules can duplicate and dispense the coded frames. So wherever the timing system fiber networks reach, all the triggers and clocks can be provided. In the experiment station hutch of BL14W1, an EVE module is equipped near the sample stage. The EVE receives the timing frames from the fiber network and gets the 125 MHz clock synchronous with the 500 MHz RF clock after decoding. The trigger pulse signal synchronized with the X-ray pulse induced by the single electron bunch can be obtained after some frequency division processing of the 125 MHz clock. The timing jitter of trigger pulses is about 6 ps and delay step of the EVE is 5 ps [17, 18].

B. Spectrometer system

The spectrometer collects photons from the sample and disperses them at different wavelengths. The PMT detects the dispersed photons and outputs electrical pulses to the DAQ system. A 0.3-m focal length triple grating imaging spectrometer (Princeton Instrument Acton SP2358), was selected. It was fitted with three gratings: 1200 lines blazed at 500 and 300 nm, and 150 lines blazed at 500 nm. The main exit port to the spectrometer is fitted with a CCD (PI-MAX3). A Hamamatsu R928 PMT, with a spectral response of 120–900 nm, is attached to the spectrometer.

To reject the dark current in the PMT, the experiment hutch shall be in darkness during the measurements, and the experimental area shall be covered with a thick aluminum foil.

C. NIM system

The NIM system explores the lifetime of XEOL according to the TCSPC principle by measuring the time difference between the timing pulse and the PMT output pulse. It includes a fast time amplifier (ORTEC-FTA820), a CFD (ORTEC-935), a TAC and single-channel analyzer (SCA) (ORTEC-567), a MCA (ORTEC-927) and a ratemeter (ORTEC-661). In the CFD, the signal is divided to two branches. In one branch the signal is inverted and delayed, while in the other branch the signal is attenuated to 20% of its original amplitude. The delay time is selected by an external cable equal to the time needed for the input pulse to rise from 20% of maximum amplitude to maximum amplitude [19]. In this measurement, the delay time is 1.7 ns. The attenuated signal is added to the inverted and delayed signal to form a bipolar signal with a zero crossing, which occurs at the time (~ 0.4 ns) when the inverted and delayed input signal rises to 20% of its maximum amplitude. The zero-crossing discriminator in the CFD detects this point and generates the corresponding timing output pulse. So the timing point is at 0.4 ns of the

leading edge of the inverted and delayed pulse, and the timing jitter is only dozens of picoseconds. To further reduce dark current count in the PMT, the CFD threshold is adjusted in advance until there are few signals from the PMT with the photon shutter closed and good signals with the shutter open. The TAC generates a linear DC voltage that is proportional to the interval between the trigger pulse from the timing system and the timing pulse from the CFD.

D. The ZnO sample

ZnO nanostructures are strong optical emitters, which are used in fast X-ray detector. ZnO has a wide bandgap (~ 3.37 eV) which leads to blue emission. The optical dynamics in ZnO nanowire reflects a ~ 400 ps lifetime in the band-gap transition [11], hence a suitable material as a sensor to detect the time structure of the storage ring. The ZnO nanowire sample was provided by Professor SUN Xu-Hui of Soochow University.

IV. RESULTS AND DISCUSSION

The measurement was carried out on Beamline BL14W1 at SSRF. The X-ray beam spot at the sample is $0.3 \text{ mm} \times 0.3 \text{ mm}$. The storage ring operates in the hybrid filling pattern with a 5 mA single bunch and 230-mA multiple bunches composed of 500 consecutive single bunches (Fig. 5). The dark time gap on both sides of the single bunch is 220 ns. The X-ray is tuned to 9.7 keV just above the K absorbed edge of the Zn element.

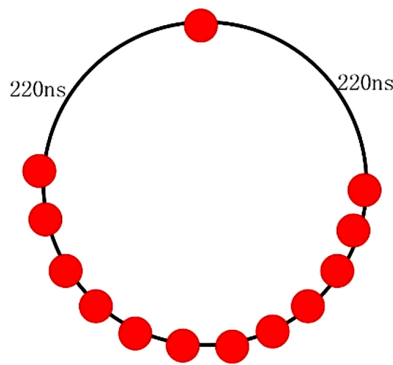


Fig. 5. (Color online) Filling pattern of the storage ring.

A. XEOL spectrum of the sample

The wavelength of the fast luminescence decay center of the ZnO must be known accurately, so as to confirm the position of spectrometer and measure time structure of the storage ring. The DAQ system collects the PMT output signal while scanning the spectrometer from 190 nm to 790 nm. The spectrum obtained is shown in Fig. 6. Two luminescence centers

can be found at 390 nm, corresponding to the ZnO bandgap luminescence, and at 500 nm, corresponding to defect structure of the ZnO nanowire.

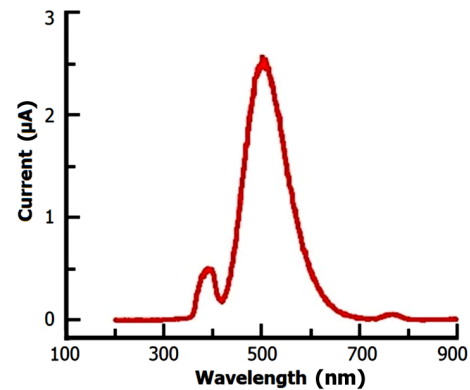


Fig. 6. (Color online) XEOL spectrum of the sample.

B. Timing mode test

There are two possible modes for timing. TAC starts by the XEOL signal and stops by the timing trigger (Mode 1), or vice versa (Mode 2). The trigger pulse rate is much higher than the luminescent signal pulse rate. The ratio factor depends on the experiment efficiency and the total dead time of the measurement setup. The two modes are of different efficiency. Decay curves (Fig. 7) were measured in both timing modes under the same condition. The results show that the measurement efficiency is much better when the XEOL signal is used as start and the timing signal as stop. In this mode, it is sure that there is a stop signal corresponding to each start signal. Otherwise, the instrument is busy all time, which will result in higher data acquisition dead time.

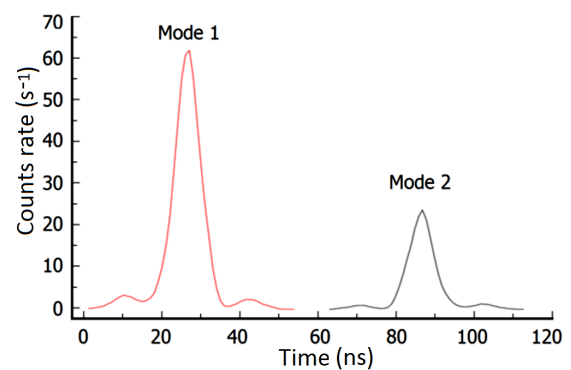


Fig. 7. (Color online) Decay curves in different timing modes.

C. The luminescent decay curve at 390 nm wavelength

The work range of TAC was set at 200 ns, the number of channels of MCA was set at 16384, so time resolution of

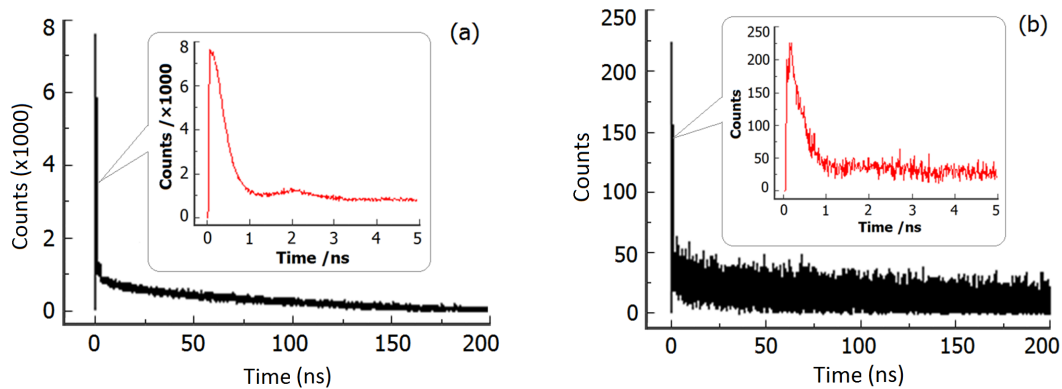


Fig. 8. (Color online) Luminescent decay curves of the sample measured in 30 min (a) and 2 min (b) at 390 nm wavelength and 12 ps time resolution.

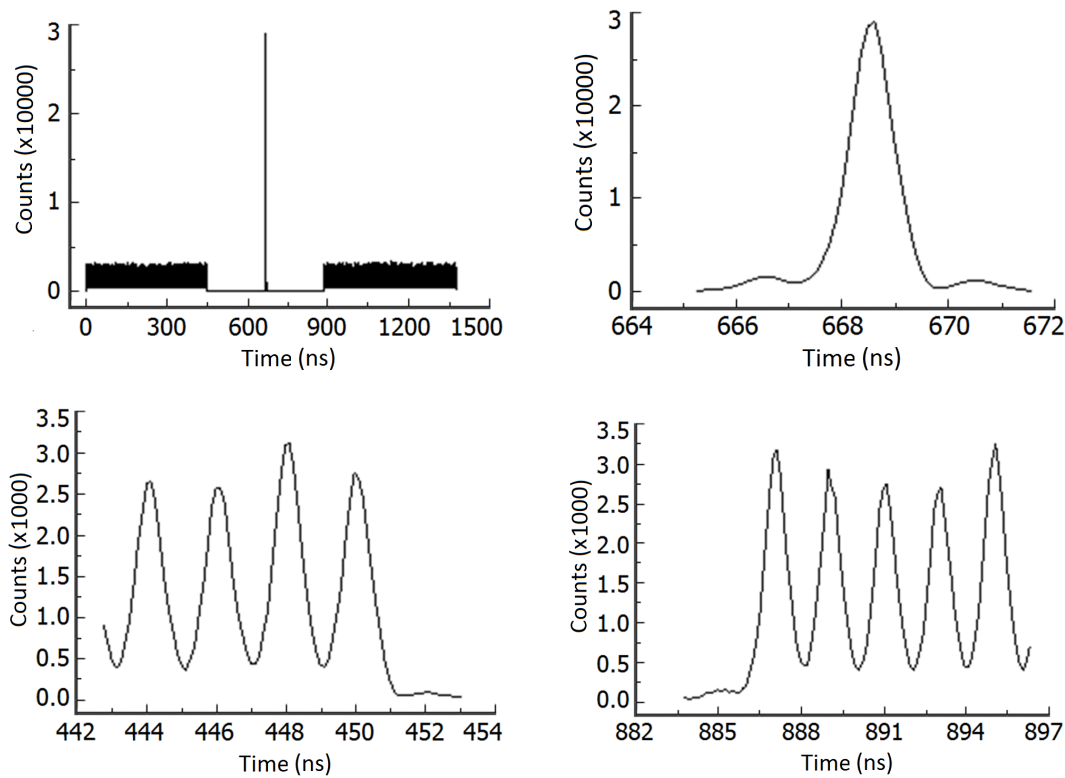


Fig. 9. Time structure of the storage ring.

the MCA was about 12 ps. The spectrometer was driven to 390 nm position. The timing was in the inversed mode. The upper decay curves measured in 30 and 2 min were shown in Fig. 8. The full width at half maximum of the dynamic process was ~ 500 ps. So the resolution of < 1 ns could be achieved with the ZnO nanowire to detect the X-ray time structure, and the signal-to-noise ratio could be improved by increasing the measurement time. Figure 8 also shows that the single bunch was impure. A weak peak can be seen at 2 ns (see the inserts). This is induced by satellite weak bunches around the single bunch. Such a single bunch can be

used to track decay events in lifetimes of nanoseconds, but it is clearly undesirable for sub-nanosecond and even shorter events [20]. The accelerator physics group of SSRF has confirmed this problem and begun to clean the single bunch.

D. Time structure of the storage ring

The work range of TAC was set at 2000 ns, which covers the 1440 ns full time scale of the storage ring. The number of MCA channels was 16 384, so the time resolution of

the MCA was about 120 ps. The spectrometer was driven to 390 nm position. The timing was in the inversed mode. Figure 9 shows the results measured in 10 min. The width of the single bunch is about 500 ps, and the dark time gap on both sides of the single bunch is 220 ns. The width of the multiple bunches is 999 ns. The data are identical to those provided by the accelerator physics group of SSRF.

V. CONCLUSION

Measuring time structure of the SSRF storage ring on the sample spot in the experimental hutch is a foundational step

during the time-resolved experiments using the pulsed synchrotron X-rays with the time structure defined by the storage ring. The traditional way is to set a fast photodiode on the sample spot to sense and record the X-ray pulses with their timestamps. A new method based on TCSCP is proposed and implemented. The measurement system has four parts: a spectrograph with PMT detector, a timing system, a set of nuclear instrument modules and a ZnO sample. The experiment results and the discussion are presented. The time resolution achieved is < 1 ns.

The measurement system can be used to make further study of the ‘pump-probe’ like timing experiments. It can also act as an experiment system for research on optical luminescent materials.

-
- [1] Tian S Q, Jiang B C, Leng Y B, *et al.* Double-mini- β_y optics design in the SSRF storage ring. Nucl Sci Tech, 2014, **25**: 030101. DOI: [10.13538/j.1001-8042/nst.25.030101](https://doi.org/10.13538/j.1001-8042/nst.25.030101)
 - [2] Milne C J, Penfold T J and Chergui M. Recent experimental and theoretical developments in time-resolved X-ray spectroscopies. Coordin Chem Rev, 2014, **277**: 44–68. DOI: [10.1016/j.ccr.2014.02.013](https://doi.org/10.1016/j.ccr.2014.02.013)
 - [3] Beiersdorfer P, Lepson J K, Bitter M, *et al.* Time-resolved x-ray and extreme ultraviolet spectrometer for use on the National Spherical Torus Experiment. Rev Sci Instrum, 2008, **79**: 10E318. DOI: [10.1063/1.2953488](https://doi.org/10.1063/1.2953488)
 - [4] Herrmann S, Hart P, Freytag M, *et al.* Diode readout electronics for beam intensity and position monitors for FELs. J Phys Conf Ser, 2014, **493**: 012014. DOI: [10.1088/1742-6596/493/1/012014](https://doi.org/10.1088/1742-6596/493/1/012014)
 - [5] Dong C Y, So P T, French T, *et al.* Fluorescence lifetime imaging by asynchronous pump-probe microscopy. Biophys J, 1995, **69**: 2234–2242. DOI: [10.1016/S0006-3495\(95\)80148-7](https://doi.org/10.1016/S0006-3495(95)80148-7)
 - [6] Lu Y Q, Zhao J B, Zhang R, *et al.* Tunable lifetime multiplexing using luminescent nanocrystals. Nat Photonics, 2014, **8**: 32–36. DOI: [10.1038/NPHOTON.2013.322](https://doi.org/10.1038/NPHOTON.2013.322)
 - [7] Reusch T, Osterhoff M, Agricola J, *et al.* Pulse-resolved multi-photon X-ray detection at 31 MHz based on a quadrant avalanche photodiode. J Synchrotron Rad, 2014, **21**: 708–715. DOI: [10.1107/S1600577514006730](https://doi.org/10.1107/S1600577514006730)
 - [8] Sham T K and Rosenberg R A. Time-resolved synchrotron radiation excited optical luminescence: Light-emission properties of silicon-based nanostructures. ChemPhysChem, 2007, **8**: 2557–2567. DOI: [10.1002/cphc.200700226](https://doi.org/10.1002/cphc.200700226)
 - [9] Liu M, Yin C X, Zhao L Y, *et al.* Design of a novel timing system. Nucl Tech, 2010, **33**: 425–428. (in Chinese)
 - [10] Becker W. Advanced time-correlated single photon counting techniques. Springer Berlin Heidelberg, 2005. DOI: [10.1007/3-540-28882-1](https://doi.org/10.1007/3-540-28882-1)
 - [11] Zhang X H, Chua S J, Yong A M, *et al.* Exciton radiative lifetime in ZnO quantum dots embedded in SiO_x matrix. Appl Phys Lett, 2006, **88**: 221903. DOI: [10.1063/1.2207848](https://doi.org/10.1063/1.2207848)
 - [12] Xu Q, Hong R D, Huang H L, *et al.* Enhanced band-gap emission in ZnO Nanocaves by two-step thermal oxidation Zn film. Mater Lett, 2013, **91**: 139–141. DOI: [10.1016/j.matlet.2012.09.042](https://doi.org/10.1016/j.matlet.2012.09.042)
 - [13] Liu H, Zhou Y, Jiang Z, *et al.* QXAFS system of the BL14W1 XAFS beamline at the Shanghai Synchrotron Radiation Facility. J Synchrotron Rad, 2012, **19**: 969–975. DOI: [10.1107/S0909049512038873](https://doi.org/10.1107/S0909049512038873)
 - [14] Vij D R. Luminescence of Solids. Springer US, 1998. DOI: [10.1007/978-1-4615-5361-8](https://doi.org/10.1007/978-1-4615-5361-8)
 - [15] Mosselmans J F W, Taylor R P, Quinn P D, *et al.* A time resolved microfocus XEOL facility at the Diamond Light Source. J Phys Conf Ser, 2013, **425**: 182009. DOI: [10.1088/1742-6596/425/18/182009](https://doi.org/10.1088/1742-6596/425/18/182009)
 - [16] Das S R and Holloway L E. Characterizing discrete event timing relationships for fault monitoring of manufacturing systems. IEEE Intl Conf Contr, 1996, 1012–1018. DOI: [10.1109/CCA.1996.559054](https://doi.org/10.1109/CCA.1996.559054)
 - [17] Vogel J, Kuch W, Bonfim M, *et al.* Time-resolved magnetic domain imaging by X-ray photoemission electron microscopy. Appl Phys Lett, 2003, **82**: 2299–2301. DOI: [10.1063/1.1564876](https://doi.org/10.1063/1.1564876)
 - [18] Zhao L Y, Yin C X and Liu D K. Application of event system in SSRF timing system. Nucl Tech, 2006, **29**: 1–5. (in Chinese) DOI: [10.3321/j.issn:0253-3219.2006.01.001](https://doi.org/10.3321/j.issn:0253-3219.2006.01.001)
 - [19] ORTEC MODEL935 manual. <http://www.ortec-online.com/download/935.pdf>
 - [20] Ego H, Hara M, Kawashima Y, *et al.* Suppression of the coupled-bunch instability in the SPring-8 storage ring. AIP Conf Proc, 1997, **413**: 267–275. DOI: [10.1063/1.54408](https://doi.org/10.1063/1.54408)